JPEDAV (2007) 28:355–361
DOI: 10.1007/s11669-007-9092-z
1547-7037 ©ASM International

The 450 °C Isothermal Section of the Zn-Fe-Ti System

Xianhui Tang, Fucheng Yin, Xinming Wang, Jianhua Wang, Xuping Su and Nai-Yong Tang

(Submitted March 15, 2006; in revised form December 13, 2006)

The 450 °C isothermal section of the Zn-Fe-Ti ternary system with an emphasis on the Zn-rich corner was experimentally determined by means of optical microscopy, scanning electron microscopic/energy-dispersive spectrometric (SEM-EDS) analysis, and x-ray diffraction. A true ternary phase T with an approximate formula of $TiFe_2Zn_{22}$ has been identified. This phase is in equilibrium with all phases in the system, except αFe, αTi, and Ti_2Zn. Four Ti-Zn binary compounds, $TiZn_{16}$, $TiZn_8$, $TiZn_3$, and TiZn, were found in this study.

Keywords phase diagram, zinc-base alloy, Zn-Fe-Ti

1. Introduction

Galvanizing Si-containing steels in unalloyed Zn baths results in excessively thick coatings with poor adhesion. This phenomenon is referred to as the Sandlin Effect in the open literature.[1-3] A practical solution to this problem is galvanizing the steels in alloyed baths. In addition to metals such as Al,[4] Ni,[5] and Mn,[6] which are currently used in the galvanizing industry, Ti is an alloying element of great potential for the galvanizing industry.[7]

Interstitial-free (IF) steels are frequently continuously galvanized for applications as exposed auto panels that are subjected to deep drawing in manufacturing. The addition of Ti to IF steels affects the kinetics of Fe-Zn phase formation in galvannealing, resulting in a more rapid growth rate of the Γ phase in the coating which, in turn, results in excessive coating powdering in panel fabrication.[8]

Hence, the information of phase equilibria in the Zn-Fe-Ti ternary system, especially in the Zn-rich corner at temperatures relevant to hot dip galvanizing, is very important to the industry. The purpose of the present study is to experimentally develop the Zn-Fe-Ti isothermal section at 450 °C, thereby generating information of importance to the galvanizing industry.

Numerous researchers have studied the Ti-Zn system, and more than 10 compounds have been reported.[9-20] However, the nature of these compounds is still a subject of discussion. Recently, Vassilev et al.[21,22] proposed a new version of the Zn-rich side of the phase diagram. These researchers believe that the intermediate phases in the system are not necessarily all line compounds and could exist in the vicinity of their respective stoichiometry, probably in metastable states. The formation of some metastable compounds was not excluded.[21]

Due to its importance to the galvanizing industry, the Fe-Zn binary system has been investigated repeatedly.[23-44] The most recent assessment of the system was carried out by Su et al.[45] The Ti-Fe phase diagram is relatively well investigated, and the version compiled by Massalski[46] will be used for the construction of the isothermal section.

Gloriant et al.[7] proposed a metastable isothermal section of the Zn-Fe-Ti ternary system at 450 °C following their experimental study of the interface layers formed on Fe and Fe-Ti alloys galvanized in molten Zn with and without Ti addition. One of the main features of the isothermal section is the presence of the large domain of the Γ_2 phase that extends well into the Zn-rich corner, coexisting with the liquid phase and all intermetallic compounds in the system. It can contain up to 12% Ti. Long annealing experiments resulted in a significant decrease in the extent of this field as equilibrium is approached. The Γ phase (Γ_1 in Gloriant's notation) was shown to possess a large composition range. It extends to the Fe-rich corner and coexists with Fe_2Ti and αFe. Only three Ti-Zn compounds, $TiZn_{15}$, $TiZn_7$, and $TiZn_3$, were detected in their study.

2. Experimental Methods

The design compositions of the alloys studied in this work are listed in Table 1. The purity of the metallic powders was 99.99 wt.%. Samples were prepared by carefully weighing the powders of Fe, Zn, and Ti, 5 g in total for each sample. All masses were weighed to an accuracy of 0.0001 g.

Some challenges were encountered while preparing the samples because of the high reactivity of Ti at elevated temperatures. In the initial trial, the Ti powder was found to react with the quartz tube, fused SiO_2 in nature, at high temperatures to form Ti oxides[22,47,48] due to the extremely negative standard Gibbs energies of formation of the oxides. As a result, the mixtures had to be contained in corundum crucibles that were then sealed in evacuated quartz capsules.

Xianhui Tang, Fucheng Yin, Xinming Wang, Jianhua Wang, and **Xuping Su,** Institute of Materials Research, School of Mechanical Engineering, Xiangtan University, Xiangtan, Hunan 411105, P.R. China; **Nai-Yong Tang,** Teck Cominco Metals Ltd., Product Technology Centre, 2380 Speak Man Drive, Mississauga, ON, Canada L5K 1B4; Contact e-mail: sxping@xtu.edu.cn

Table 1 Alloy and phase compositions

			Composition, at.%		
	Design composition	Phase	Ti	Fe	Z n
1	93Zn-4.5Ti-2.5Fe	$TiZn_{16}$	5.7	0.2	94.1
		T	3.8	6.0	90.2
		ηZn	0.4	0.0	99.6
2	93Zn-1.5Ti-5.5Fe	ηZn	0.0	0.5	99.5
		ζ	0.4	6.0	93.6
		T	3.9	7.7	88.4
3	93Zn-0.5Ti-6.5Fe	ζ	0.2	6.8	93.0
4	91Zn-7Ti-2Fe	$TiZn_{16}$	5.8	0.0	84.2
		$TiZn_8$	10.1	0.4	89.4
		T	4.4	6.3	89.3
5	91Zn-4.5Ti-4.5Fe	$TiZn_{16}$	5.8	0.1	94.1
		T	4.0	6.0	90.0
6	91Zn-1.5Ti-12Fe	T	3.9	8.2	87.9
		δ	1.0	7.8	91.1
		ζ	0.3	6.6	93.1
7	91.5Zn-1Ti-7.5Fe	δ	0.6	7.7	91.7
8	90.5Zn-Ti2-7.5Fe	ζ	0.2	6.6	93.2
		T	3.9	7.9	88.2
9	90Zn-4Ti-6Fe	ηZn	0.0	0.7	99.3
		T	3.8	6.0	90.2
10	87.5Zn-1Ti-11.5Fe	δ	1.1	11.0	87.8
11	87Zn-10Ti-3Fe	$TiZn_8$	10.5	0.3	89.2
		T	4.4	6.7	88.9
12	86.5Zn-1.5Ti-12Fe	T	4.1	8.6	87.3
		δ	0.7	12.0	87.2
		Γ_1	0.8	16.6	82.6
13	86Zn-1Ti-13Fe	Γ_1	1.0	18.2	80.8
		δ	0.3	12.6	87.1
14	80Zn-15Ti-5Fe	$TiZn_8$	10.9	0.8	89.3
		$TiZn_3$	22.3	0.6	77.1
		T	4.3	7.2	88.5
15	80Zn-2.5Ti-17.5Fe	Γ	0.8	24.5	74.7
		Γ_1	0.8	19.6	79.6
		T	4.0	9.0	87.0
16	78.5Zn-2Ti-19.5Fe	Γ	74.9	0.8	24.3
		T	4.5	8.7	86.8
17	73Zn-26Ti-1Fe	$TiZn_3$	23.4	0.8	75.8
		TiZn	48.3	0.6	51.1
		T	4.6	7.3	88.1
18	70Zn-15Ti-15Fe	$TiFe_2$	32.3	65.5	2.2
		TiFe	48.3	50.5	2.2
		T	4.9	8.0	87.1
19	70Zn-13.5Ti-16.5Fe	TiFe	48.9	49.1	2.0
		T	4.8	8.0	87.2
20	70Zn-10Ti-20Fe	$TiFe_2$	31.1	66.1	2.8
		T	4.5	8.4	87.1
21	65Zn-20Ti-15Fe	TiFe	50.2	49.2	0.6
		TiZn	49.4	1.1	49.4
		T	4.8	7.7	87.5

Each alloy mixture was heated to above its estimated liquidus temperature and kept at this temperature for 14 h, followed by quenching in water using a bottom-quenching technique to minimize Zn loss and to reduce sample porosity. This technique has been reported elsewhere[49,50] and will not be detailed here. The quenched samples, together with their corundum crucibles, were then sealed again individually in evacuated quartz tubes and annealed at 450 °C for 30 days to ensure the establishment of an equilibrium state. The treatment was completed with rapid water quenching to preserve the equilibrium state at 450 °C.

The specimens were prepared in the conventional way for microstructure examination using both optical and scanning electron microscopes (SEM). A nital solution was used to reveal the microstructures of the samples. A JSM-6360LV scanning electron microscope (SEM) equipped with an OXFORD INCA energy dispersive X-ray spectroscope (EDS) was used to study the morphology and chemical compositions of various phases in the samples. The phase makeup of the alloys was further determined by analyzing x-ray diffraction patterns generated by a Bruker D8 advanced x-ray diffractometer, operating at 50 kV and 100 mA with Cu K α radiation.

3. Results and Discussion

Phases in an alloy can be easily differentiated based on the relief, color, and chemical composition. In most cases, the results obtained by SEM-EDS analysis alone are sufficient for phase identification; however, the true identities of the phases were all confirmed by analyzing the relevant x-ray diffraction patterns.

All phases found in the alloys are listed in Table 1 (Column 3) together with the chemical compositions determined by the SEM-EDS technique (Columns 4 to 6). The compositions reported are the averages over at least five measurements. An important discovery of this study is that the T phase, which was believed previously to be the extension of the Γ_1 phase[7] of the binary Zn-Fe system, is a true ternary phase existing in a separate composition range. As can be seen in Fig. 1(a), the microstructure of Alloy 15 (Zn-2.5Ti-17.5Fe) consisted of three phases: T, Γ, and Γ_1. These three phases can be easily differentiated based on their morphology, relief, and chemical compositions. The T phase is most resistant to etching among the three. SEM-EDS analyses revealed that the T phase contained 4.0% Ti, 9.0% Fe, and 87.0% Zn (all compositions in at.% except if otherwise noted). This composition is markedly different from the chemical composition of the Γ_1 phase of 0.8% Ti, 19.6% Fe, and 79.6% Zn. Indexing of the x-ray diffraction pattern generated from this alloy, as shown in Fig. 1(b), indicates clearly that this alloy consisted of three phases with the T phase possessing its own set of characteristic peaks. The microstructure and x-ray diffraction pattern of Alloy 9 are shown in Fig. 2(a) and (b), respectively. It can be seen very clearly that the microstructure of this alloy consists of two phases: the T phase and the Zn-rich solid-solution phase ηZn, marked as "Liquid" in the figure because it was in the liquid state at 450 °C. It should be mentioned that the ηZn is apparently supersaturated with Ti and Fe. All three strongest peaks of this phase shifted noticeably in Fig. 2(b). Judging by the positions of the (002)

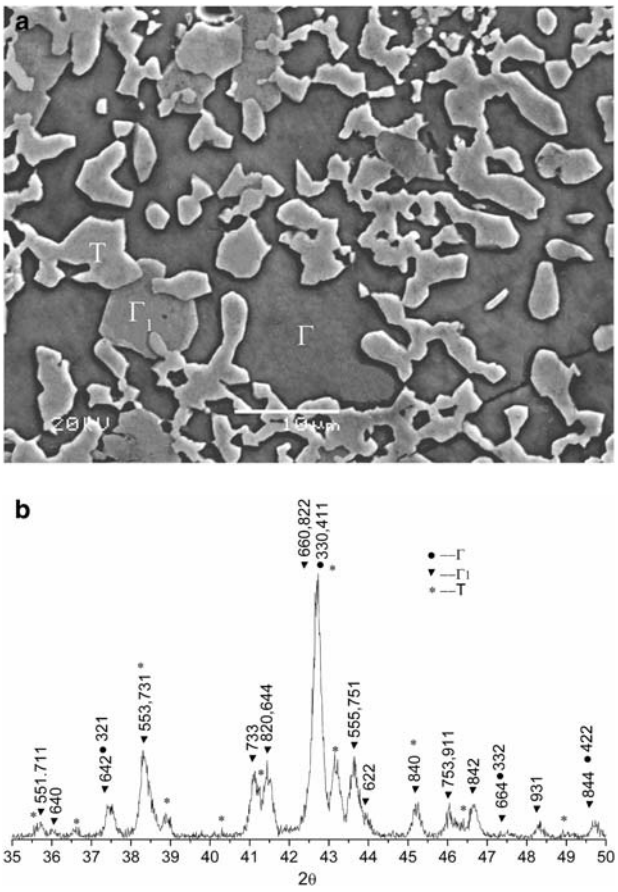

Fig. 1 The microstructure (a) and x-ray diffraction pattern (b) of Alloy 15. The composition, the morphology, and the characteristic x-ray diffraction peaks of the T phase indicate that it is a true ternary phase

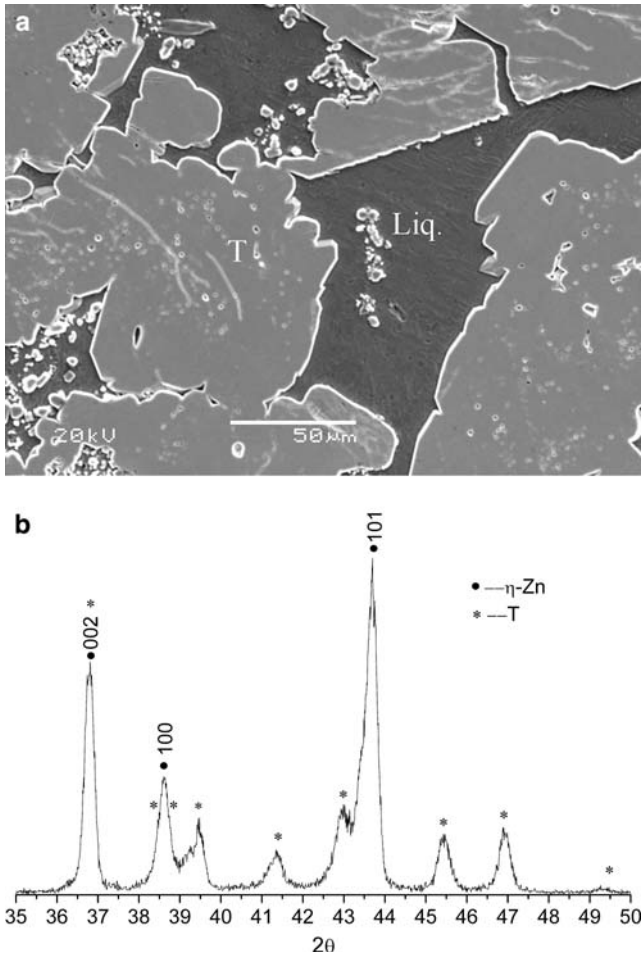

Fig. 2 The microstructure (a) and x-ray diffraction pattern (b) of Alloy 9. Note the ηZn (marked as Liq.) is supersaturated with Ti and Fe, as indicated by the noticeable shifts of its major peaks in the x-ray pattern

and (100) reflections, lattice parameter a increased and c decreased. The characteristic peaks of the T phase can be seen clearly in Fig. 2(b) because T phase is the major phase in Alloy 9. A comparison of the x-ray patterns shown in Fig. 1(b) and 2(b) indicates very clearly that the x-ray pattern of the T phase is vastly different from that of the Γ_1 phase. The Γ_1 phase is well studied. It possesses a face-centered cubic (fcc) crystallographic structure with $a = 1.798$ nm, and the unit cell contains 408 atoms. Its strongest peak is at $2\theta = 42.64°$. On the other hand, the patterns shown in Fig. 1(b) and 2(b) suggest that the strongest peak of the T phase is at $2\theta = 43°$.

The data listed in Table 1 indicate that the T phase has a relatively narrow composition range. It contains Ti from 3.8 to 4.9%, Fe from 6.0 to 7.3%, and Zn from 87.1 to 90.2%. The average composition of all T particles analyzed in this work suggests this compound can be approximately described by the formula of $TiFe_2Zn_{22}$. Ternary phases were frequently detected in the Zn-rich corner of Zn-Fe-based ternary systems, such as the Zn-Fe-Al system,[51] the Zn-Fe-Co system,[49] and the Zn-Fe-Ni system.[52] These phases all have the same fcc crystallographic structure and the same size of unit cell. These phases were all designated as T phase by Tang.[49,51,52] To be consistent, this phase is also designated as T.

SEM-EDS analyses indicate that the microstructure of Alloy 12 (Zn-1.5Ti-12Fe) corresponded to the $(T + \Gamma_1 + \delta)$ three-phase equilibrium state. The relief and compositions of the T phase and the Γ_1 phase were significantly different.

The microstructures of Alloys 5, 8, 11, and 13 were quite simple and consisted of two phases (see Table 1 for details) with the minor phase existing in the matrix of the major phase. Their microstructures are similar to that shown in Fig. 2(a) for Alloy 9.

The microstructure and the x-ray diffraction pattern of Alloy 2 are shown in Fig. 3(a) and (b). SEM-EDS analyses indicate that it corresponded to the $(T + \zeta + \eta Zn)$ three-phase equilibrium state. Ti was practically not detected in the ηZn phase. A separate study carried out by one of the authors indicated that the Ti composition of this invariant point at 450 °C is only 0.03 wt.%.[53] It can be seen that the lattice of the ηZn phase was not noticeably distorted in this

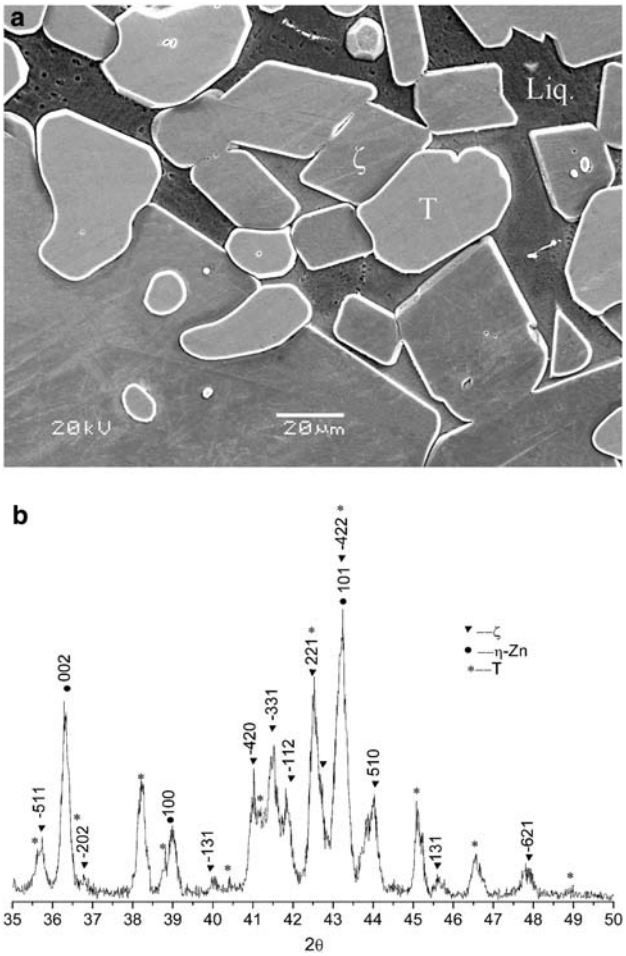

Fig. 3 The microstructure (a) and x-ray diffraction pattern (b) of Alloy 2. Three phases, T, ζ, and ηZn, coexist in this alloy

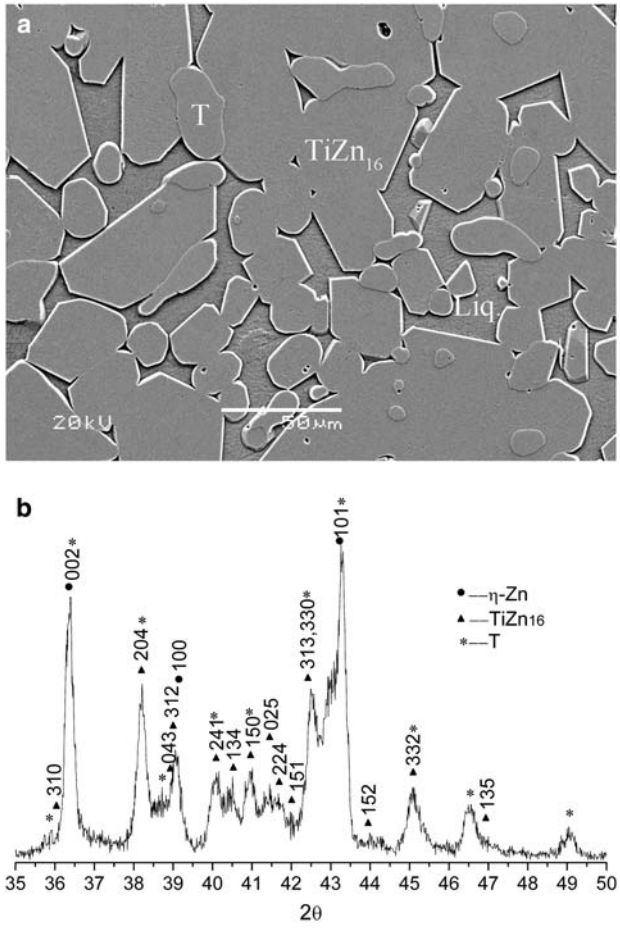

Fig. 4 The microstructure (a) and x-ray diffraction pattern (b) of Alloy 1. Three phases, $TiZn_{16}$, T, and ηZn, coexist in this alloy

case; the three peaks of this phase are located at their normal positions as shown in Fig. 3(b). Based on the fact that the ηZn phase in Alloy 2 contained more Fe and less Ti than that in Alloy 9,[53] one can conclude that the lattice distortion of the ηZn phase in Alloy 9 was mostly caused by Ti supersaturation.

The microstructure of Alloy 1 (Zn-4.5Ti-2.5Fe) is shown in Fig. 4(a). The phases existing in this alloy were identified as T, $TiZn_{16}$, and ηZn. The designation of $TiZn_{16}$ is based on the x-ray diffraction pattern of the compound. The existence of $TiZn_{16}$ is first reported by Heine who published the x-ray diffraction pattern of this compound.[14] This compound has been included in the phase diagram proposed recently by Vassilev.[22] The presence of this phase at 450 °C substantiates the early finding that the peritectic temperature of its formation is 460 °C,[10,11] higher than the 445 °C indicated by Massalski.[46] The T phase is more resistant to etching than the $TiZn_{16}$.phase. As a result, it is easy to distinguish the T phase from the $TiZn_{16}$ phase based on their relief and compositions. The x-ray diffraction pattern of Alloy 1 is shown in Fig. 4(b). SEM-EDS analysis indicated that the solubility of Fe in $TiZn_{16}$ is small, no more than 0.3%. Figure 5 shows the microstructure (Fig. 5a) and x-ray diffraction pattern (Fig. 5b) of Alloy 4 (Zn-7Ti-2Fe). It corresponds to the ($TiZn_{16}$ + $TiZn_8$ + T) three-phase equilibrium state. Again, the Fe solubility in $TiZn_{16}$ is negligible.

As indicated earlier, the prevailing Zn-Ti phase diagram[9] includes $TiZn_{10}$ and $TiZn_5$, but not $TiZn_8$. The diffraction patterns of Alloys 4 and 14 shown in Fig. 5(b) and 6(b), were carefully studied. With the removal of all peaks contributed by phases T, $TiZn_{16}$, and $TiZn_3$, the remaining peaks in the two patterns are consistent. This indicated that only one phase exists between the $TiZn_{16}$ and $TiZn_3$ phases. Energy-dispersive spectrometric analysis in Table 1 indicates that the phase is $TiZn_8$. A similar phase with a composition corresponding to $TiZn_7$ was identified in the work of Gloriant et al.[7] Chen et al.[54] reported the existence of Ti_3Zn_{22} and determined the crystal structure in detail. The exact composition of this phase is $Ti_{2.841}Zn_{22.159}$, which corresponds to the $TiZn_8$ phase. Most likely, these two phases are the same, although Vassilev[22] suggested recently the existence of both $TiZn_7$ and $TiZn_8$. The minor

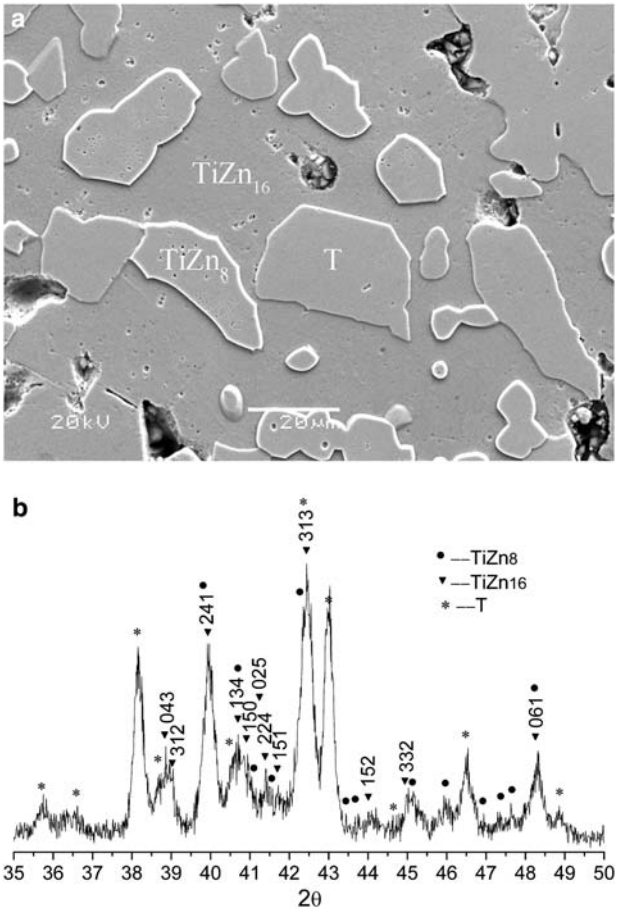

Fig. 5 The microstructure (a) and the x-ray diffraction pattern (b) of Alloy 4. Three phases, $TiZn_{16}$, $TiZn_8$, and T, coexist in this alloy

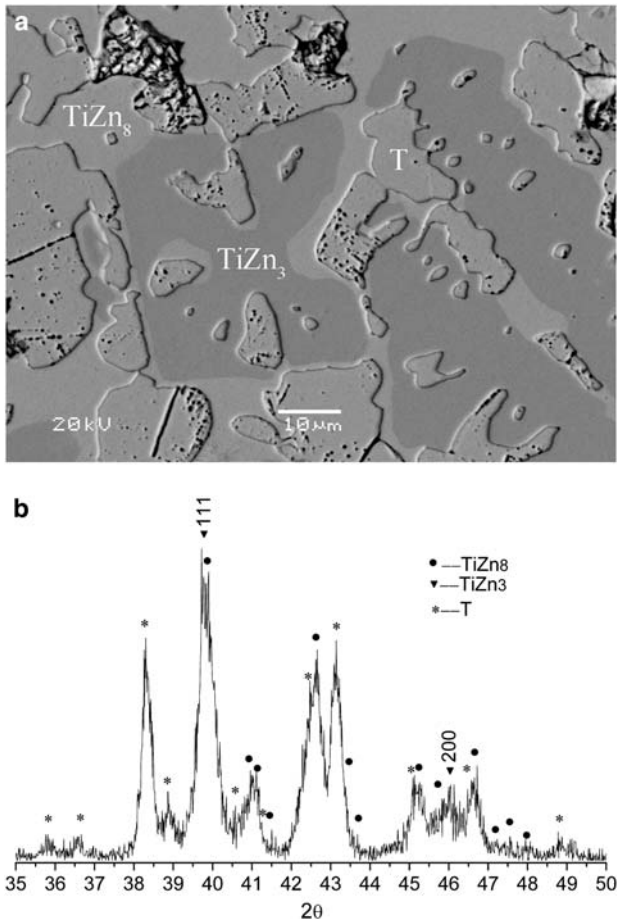

Fig. 6 (a) The microstructure of Alloy 14 consists of the following three phases, $TiZn_8$, $TiZn_3$, and T. These three phases possess totally different relief and can be easily differentiated in this backscattered electron (BSE) micrograph. (b) The x-ray diffraction pattern of Alloy 14

difference in composition of the two phases could be the result of the uncertainty associated with SEM-EDS analysis. In the present work, the results of Chen et al. are accepted. The $TiZn_8$ compound dissolved about 0.4 to 0.8% Fe, more than that of the $TiZn_{16}$ compound.

The microstructure of Alloy 17 is shown in Fig. 7. It consists of the T phase, the TiZn phase, and the $TiZn_3$ phase. The existence of this phase field makes the equilibrium between the FeTi phase and the $TiZn_3$ phase, as suggested by Gloriant et al.,[7] impossible.

During the annealing, samples of Alloy 18 to Alloy 21 often expanded significantly and even became powder presumably because there was no liquid phase acting as the binding phase, and intermetallic phases of Fe-Ti types are brittle in nature. It was difficult to obtain compact samples. SEM-EDS analyses of these porous samples suggest the existence of (TiFe + TiZn + T), (TiFe + $TiFe_2$ + T), and ($Fe_2Ti + \alpha Fe + T$) three-phase equilibrium fields in these samples. The maximum solubility of Zn in FeTi and Fe_2Ti is about 2.8% and 2.2%, respectively. Because of the small volume fractions of the FeTi and the Fe_2Ti phases in the samples, it is difficult to identify their characteristic peaks with any certainty in the x-ray diffraction patterns.

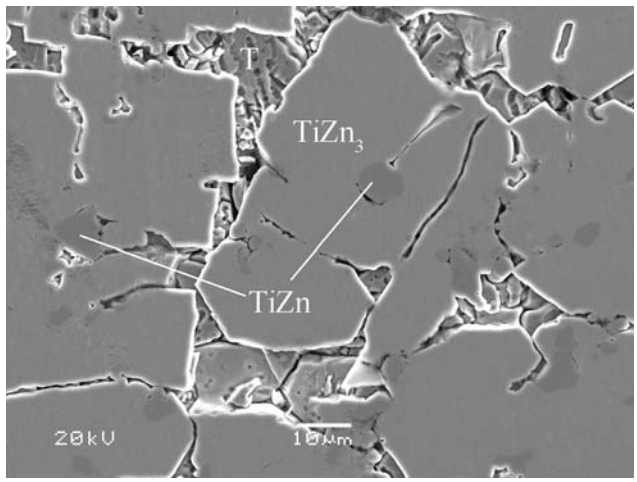

Fig. 7 Three phases, T, $TiZn_3$, and TiZn, coexist in Alloy 17. Note that TiZn particles are smaller, darker, and totally surrounded by large $TiZn_3$ particles

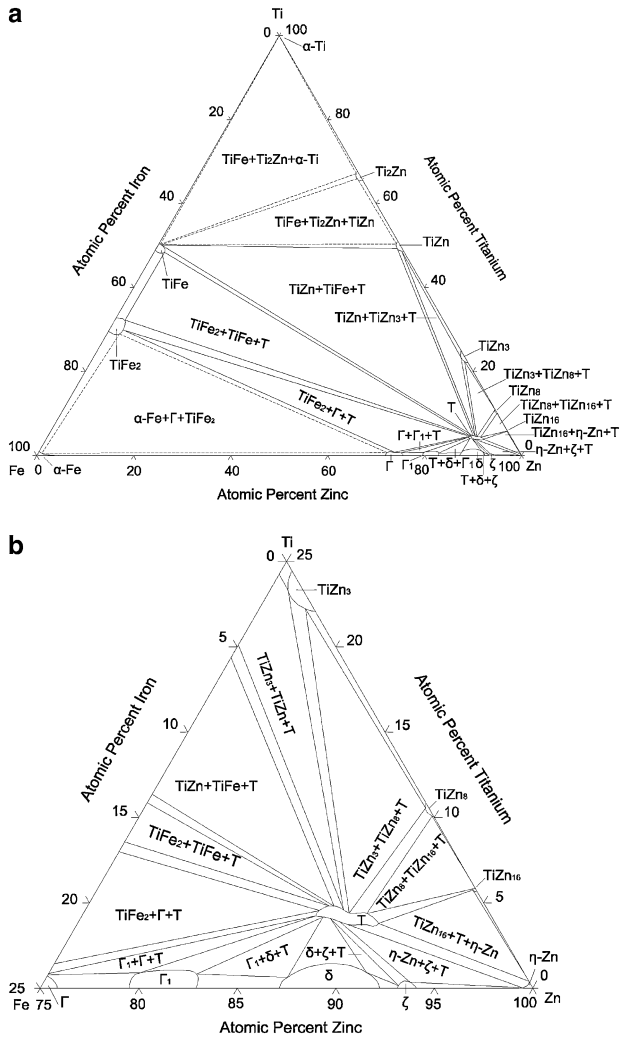

Fig. 8 The 450 °C isothermal section of the Zn-Fe-Ti system (a) and the enlarged Zn-rich corner (b)

Based on the experimental results obtained in this study and the information of relevant binary systems in the open literature, the 450 °C isothermal section is constructed, as shown as Fig. 8(a). An enlarged Zn-rich corner is shown in Fig. 8(b). It should be mentioned here that only four Ti-Zn compounds-namely, $TiZn_{16}$, $TiZn_8$, $TiZn_3$, and TiZn-were found in the present investigation. Other Ti-Zn compounds, such as $TiZn_5$, $TiZn_{10}$, $TiZn_2$, and Ti_2Zn_3, as shown in the prevailing Ti-Zn binary phase diagram proposed by Massalski,[9] were not detected in the present study. It can be seen in the isotherm that the T phase is in equilibrium with ηZn, ζ, δ, Γ_1, Γ, Fe_2Ti, FeTi, TiZn, $TiZn_3$, $TiZn_8$, and $TiZn_{16}$. The existence of the (TiZn + T + $TiZn_3$) three-phase equilibrium state prohibits the equilibrium between FeTi and $FeZn_3$ suggested by Gloriant et al.[7] The composition range of the T phase is relatively small and narrow. With an increase in the Zn content of the T phase, the Ti content of the phase changes only marginally. As a result, the T phase field is almost parallel to the Fe-Zn binary side of the system.

4. Conclusions

Based on SEM-EDS analyses and x-ray diffraction studies, the 450 °C isothermal section of the Zn-Fe-Ti ternary system was determined in the present work. The main findings are:

- The T phase is a true ternary phase. It can be described approximately by the formula $TiFe_2Zn_{22}$. The composition range of the T phase is relatively small.
- The ternary phase T is in equilibrium with all the phases in the system except αFe, αTi, and Ti_2Zn.
- The equilibrium between the TiZn, T, and $TiZn_3$ phases prohibited the equilibrium between FeTi and $FeZn_3$ compounds, as suggested by others.[7]
- There were only the following four Ti-Zn compounds, $TiZn_{16}$, $TiZn_8$, $TiZn_3$, and TiZn found in present work.

Acknowledgment

This investigation was supported by the National Science Foundation of China (No. 50471064) and Program for New Century Excellent Talents in University (NCET-04-778).

References

1. T.W. Sandelin, *Wire Wire Prod.*, 1940, **11**, p 655
2. J. Foct, P. Perrot, and G. Reumont, Interpretation of the Role of Silicon on the Galvanizing Reaction Based on Kinetics, Morphology and Thermodynamics, *Scr. Metall. Mater.*, 1993, **28**, p 1195
3. H. Guttman and P. Niessen, *Reactivity of Silicon Steels in Hot-Dip Galvanizing, Can. Metall. Quart.*, 1972, **11**, p 609
4. A.R.P. Ghuman and J.L. Goldstein, Reaction Mechanisms for the Coatings Formed During the Hot Dipping of Iron in 0 to 10 pct Al-Zn baths at 450 to 700 °C, *Metall. Trans.*, 1971, **2**, p 2903
5. A.F. Skenazi and D. Rollez, Hot Dip Galvanizing of Semi-Killed Steels with the Zinc-Nickel Bath, *Proc. 15th International Galvanizing Conference*, GE2/1-5, 1988
6. G. Reumont, J.C. Tissier, and J.Y. Dauphin, Morphology, Structure and Formation Conditions of Drosses in Hot Dip Galvanizing Nickel-Added Baths, *Métall.*, 1989, **86**, p 799
7. T. Gloriant, G. Reumont, and P. Perrot, The Fe-Zn-Ti system at 450°C, *Z. Metallkd.*, 1997, **88**(7), p 539
8. A.R. Marder, The Metallurgy of Zinc-Coated Steel, *Prog. Mater. Sci.*, 2000, **45**, p 191-271
9. T.B. Massalski, Zn-Ti Phase Diagram, *Binary Alloy Phase Diagrams*, 1990, **3**, p 3501
10. E. Gebhardt, *Z. Metallkd.*, 1941, **33**, p 355
11. E.A. Anderson, E.J. Boyle, and P.W. Ramsey, *Trans. AIME*, 1944, **156**, p 278
12. P. Pietrokowsky, *Trans. Met. Soc. AIME*, 1954, **200**, p 219
13. M.E. Pelzel, *Metallography*, 1961, **15**, p 881
14. W. Heine and U. Zwicker, *Z. Metallkd.*, 1962, **53**, p 380
15. K. Schubert, K. Frank, R. Gohle, A. Maldonado, H.G. Meissner, A. Raman, and W. Rossteutscher, *Naturwissenschaften*, 1963, **50**, p 41
16. E.H. Rennhack, *Trans. Metall. Soc. AIME*, 1966, **236**, p 941

17. J.A. Spittle, Effects of Composition and Cooling Rate on the As-Cast Microstructures of Zn-Ti Alloys, *Metallography*, 1972, **5**, p 423
18. R. Dobrev, V. Dimova, and I. Georgiev, *Mater. Tehnologia*, 1977, **5**, p 40
19. S. Goto, K. Esashi, S. Koda, and S. Morozumi, Structure-Controlling of Zn-Ti Hyper-Eutectic Alloys by Unidirectional Solidification, *J. Jpn. Inst. Met.*, 1973, **37**, p 466
20. M. Saillard, G. Develey, C. Becle, J.M. Moreau, and D. Paccard, The Structure of $TiZn_{16}$, *Acta Crystallogr. B*, 1981, **37**, p 224
21. G.P. Vassilev, X.J. Liu, and K. Ishida, Reaction Kinetics and Phase Diagram Studies in the Ti-Zn System, *J. Alloy. Compd.*, 2004, **375**, p 162
22. G.P. Vassilev, Contribution to the Zinc-Rich Side of the Ti-Zn System, *Z. Metallkd.*, 2004, **95**(9), p 813
23. J. Schramm, *Z. Metallkd.*, 1936, **28**(7), p 203
24. E.C. Truesdale, R.L. Wilcox, and J.L. Rodda, *Trans. Met. Soc. AIME*, 1936, **122**, p 192
25. M. Fallot, *Ann. Phys.*, 1937, **7**, p 420
26. J. Schramm, *Z. Metallkd.*, 1937, **29**(7), p 222
27. P.J. Brown, The Structure of the δ-phase in the Transition Metal-Zinc Alloy System, *Acta Crystallogr.*, 1962, **15**, p 608
28. G.R. Speich, L. Swell, and H.A. Wriedt, *Trans. Met. Soc. AIME*, 1964, **230**, p 939
29. H.A. Wriedt and S. Arajs, *Phys. Stat. Solidi*, 1966, **16**, p 475
30. H.A. Wriedt, *Trans. Met. Soc. AIME*, 1967, **239**, p 1120-1128
31. A. Johannsson, H. Ljung, and H. Westman, *Acta Chem. Scand.*, 1968, **22**, p 2743
32. V-S Budurov, P. Kovatchev, N. Stojcev, and Z. Kamenova, Iron Side of the Fe-Zn Phase Diagram, *Z. Metallkd.*, 1972, **63**(6), p 348
33. G. Kirchner, H. Harvig, K.R. Moquist, and M. Hillert, Distribution of Zinc Between Ferrite and Austenite and the Thermodynamics of the Binary Fe-Zn System, *Arch. Eisenhuttenwes.*, 1973, **44**(3), p 227
34. G.F. Bastin, F.J.J. Van Loo, and G.D. Riek, New Compound in the Iron-Zinc System, *Z. Metallkd.*, 1974, **65**, p 656
35. J.K. Brandon, R.Y. Brizard, P.C. Chieh, R.K. McMillian, and W.B. Pearson, New Refinements of the γ Brass Type Structures Cu_5Zn_8, Cu_5Cd_8 and Fe_3Zn_{10}, *Acta Crystallogr.*, 1974, **B30**, p 1412
36. P.J. Gellings, E.W. de Bree, and G. Gierman, *Z. Metallkd.*, 1979, **70**(5), p 315
37. T. Nishizawa, M. Hasebe, and M. Ko, Thermodynamic Analysis of Solubility and Miscibility Gap in Ferromagnetic Alpha Iron Alloys, *Acta Metall.*, 1979, **27**, p 817
38. P.J. Gellings, G. Gierman, D. Koster, and J. Kuit, *Z. Metallkd.*, 1980, **71**(2), p 70
39. A.S. Koster and J.C. Schoone, Structure of the Cubic Iron-Zinc Phase $Fe_{22}Zn_{78}$, *Acta Crystallogr.*, 1981, **B37**, p 1905
40. M. Tomita, T. Azakami, L.M. Timberg, and J.M. Toguri, Thermodynamics of the Fe-Zn System, *Trans. Jpn. Inst. Met.*, 1981, **22**, p 717
41. S. Peterson, P.J. Spencer, and K. Hack, *Thermochim. Acta*, 1988, **129**, p 77
42. P. Perrot and J.Y. Dauphin, Calculation of the Fe-Zn-Si Phase Diagram Between 773 and 1173 K, *Calphad*, 1988, **12**, p 33
43. M. Hamalainen, R. Luoma, and P. Taskinen, TKK-V-B55, Helsinki University of Technology, Espoo, Finland, 1990
44. G. Reumont, P. Perrot, J.M. Fiorani, and J. Hertz, Thermodynamic Assessment of the Fe-Zn System, *J. Phase Equilibria*, 2000, **21**, p 371
45. X. Su, N.-Y Tang, and J.M. Toguri, Thermodynamic Evaluation of the Fe-Zn System, *J. Alloy. Compd.*, 2001, **325**, p 129
46. T.B. Massalski, Ti-Fe Phase Diagram, *Binary Alloy Phase Diagrams*, 1990, **2**, p 1785
47. R. Swalin, *Thermodynamics of Solids*. Wiley, London, 1961, p 316
48. I. Barin, *Thermochemical Data of Pure Substances, Part II*. VCH Verlags, Weinheim, 1993, p 1739
49. N.-Y Tang, X. Su, and J.M. Toguri, Experimental Study and Thermodynamic Assessment of the Zn-Fe-Ni System, *Calphad*, 2001, **25**, p 267
50. X. Su, N.-Y Tang, and J.M. Toguri, 450°C Isothermal Section of the Fe-Zn-Si Ternary Phase Diagram, *Can. Metall. Q.*, 2001, **40**, p 377
51. N.-Y Tang and X. Su, On the Ternary Phase in the Zinc-Rich Corner of the Zn-Fe-Al System at Temperatures Below 450°C, *Metal. Mater. Trans.*, 2002, **33A**, p 1559
52. N.-Y Tang, X. Su, and X. Yu, The Zn-Rich Corner of the Zn-Fe-Co System at 450°C, *Z. Metallkd.*, 2003, **94**(2), p 116
53. N.-Y. Tang, Unpublished research work
54. X.A. Chen, W. Jeitschko, M.E. Danebrock, C.B.H. Evers, and K. Wangner, Preparation, Properties, and Crystal Structures of Ti_3Zn_{22} and $TiZn_{16}$, *J. Solid State Chem.*, 1995, **118**, p 219